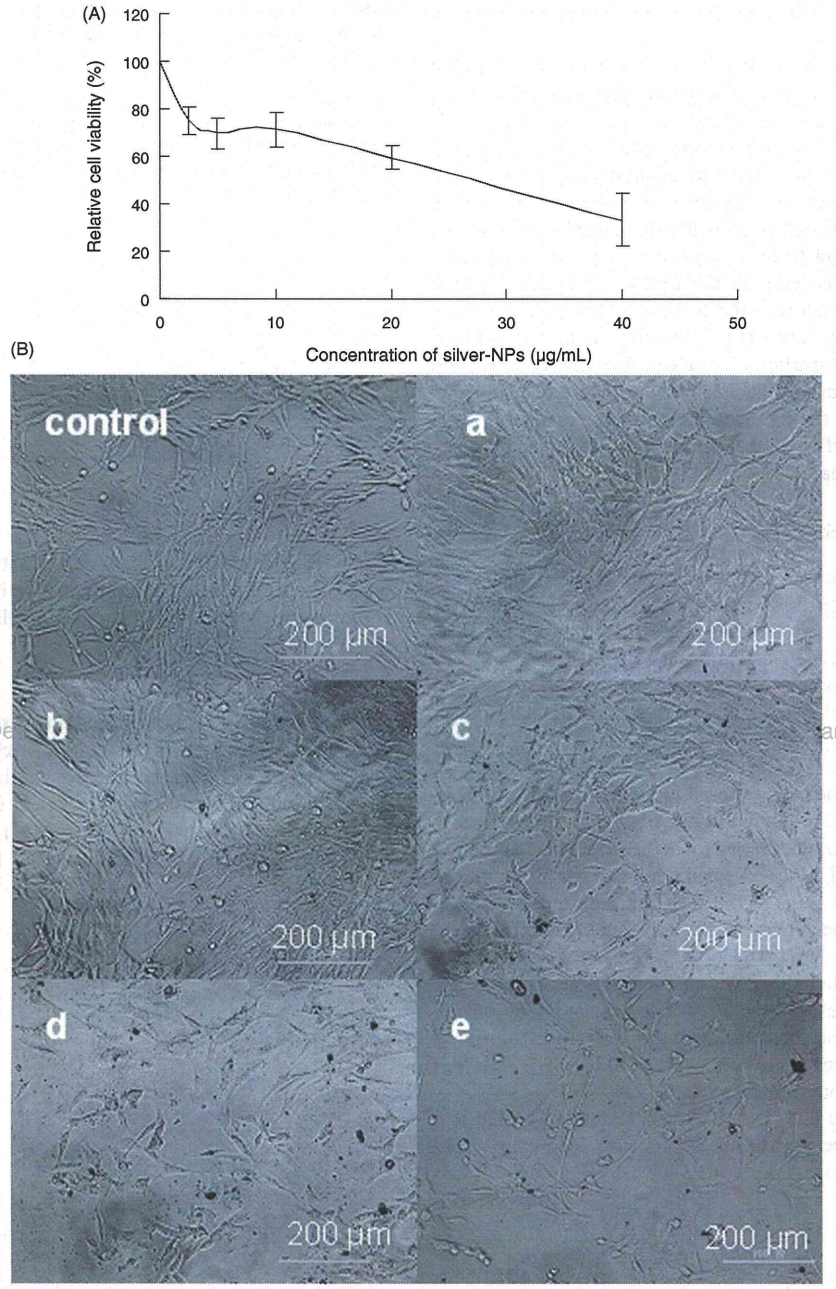

Fig. 2. (a) Relative viability and (b) morphological changes in SHE cells after exposure to different doses of silver-NPs. A relative viability curve was generated from MTT assay. The morphological changes of the cells were observed using light microscopy. Control: untreated cells; (a)–(e): cells exposed to silver-NPs (2.5, 5, 10, 20, and 40 μg/mL), respectively. Magnification: $\times$ 200.

45.7% 59.9–100.9 nm; 40.9% 100.1–189.1 nm; 9% 818.4–1009.0 nm (Fig. 1(d)). The variations in size may be attributable to changes in the hydrodynamic radii of the particles in the different media, which may in turn be due to particle and media interactions. The larger particles (over 100 nm in diameter) were observed in both distilled water and cell culture media (Figs. 1(c) and (d)). This may be due to particle agglomeration upon dispersal in the

media. DLS may indicate the hydrodynamic radius rather than particle size.

The average zeta potential, as measured at silver-NP concentrations of 40, 100, and 1000 ppb were found to be −22.0, −26.4, and −29.8 mV in water and −8.2, −9.2, and −8.76 mV in cell culture media (Fig. 1(e)). Zeta potential values of this nature suggest that, upon dispersion, the particles form an unstable dispersal pattern. The average zeta potentials in cell culture media with silver-NPs were found to be dramatically different from those of silver-NP dissolved in distilled water, suggesting that silver-NPs interact with the components of the cell culture media. This in turn suggests significant protein adsorption by the nanoparticles in the cell growth media. Protein adsorption from the medium is also reflected in the size distribution of the particles, as determined by DLS. This may have an effect on the cellular response to the presence of silver nanoparticles.

3.2. Cytotoxicity

A relative viability curve was generated from MTT assay (Fig. 2(a)). The 50% inhibition concentration (IC_{50}) of silver-NPs exposed to SHE cells for 24 h was estimated on the basis of the MTT assay results. The relative cell viability decreased as the concentration of silver-NPs increased (Fig. 2(a)). Relative inhibition rate of SHE cells which were exposed to silver-NPs at 0, 2.5, 5, 10, 20, and 40 μg/mL were 0, 24.87, 30.37, 28.69, 40.40 and 66.63%, respectively. The cells exposed to the 2.5 μg/mL of silver-NPs had a relative inhibition rate of over 20%, but no significant morphological changes. When the cells exposed to the 5 μg/mL of silver-NPs had a relative inhibition rate of about 30% and some of the cells appeared to have shrunk (Fig. 2(b)). The growth was significantly inhibited when the cells exposed to the 10 or 20 μg/mL of silver-NPs, and had a relative inhibition rate of over 40% at 20 μg/mL of silver-NPs exposure (Fig. 2(b)). The relative inhibition rate was then estimated at different concentrations of silver-NPs. The IC_{50} of silver-NPs exposed to the SHE cells was estimated on the basis of $\lg IC_{50} = Xm - I(P - (3 - Pm - Pn)/4)$ to be 15.24 μg/mL. These results suggested that silver-NPs have significant cytotoxicity to primary SHE cells, even at low doses.

3.3. Genotoxicity

Chromosome damage was detected in primary SHE cells exposed to silver-NP using a CBMN assay. These data are expressed as the rate of micronucleation per 1000 BNCs per culture. Cells treated with MMC (positive control) showed an MNF of 7.67% (Table I, Fig. 3). Cells treated with NaCl (negative control) showed an MNF of 1.6%, and the difference was found to be significant ($P < 0.05$). There was a significant increase ($P < 0.05$) in the frequency of MN for all cells exposed to silver-NPs (Table I, Fig. 3).

Table I. Micronucleation frequency (MNF (%)) of SHE cells treated with MMC (positive control), NaCl (negative control), and silver-NP. The micronucleation frequency was determined for 1000 binucleated cells (BNCs) per culture and in a total 3000 BNCs per concentration. The significance of the difference between the positive control and the negative control was determined using t-testing; and the significance of all test samples relative to the negative control was identified using one-way ANOVA and Dunnett tests (2-sided). *, $P < 0.05$. The data represent the mean ± SD ($n = 3$).

				95% confidence interval of the mean	
Test	Dose	FMN (%)	P-value	Lower bound	Upper bound
NaCl (sol.)	50 μL/mL	1.6 ± 0.66		−0.029	3.229
	10 μg/mL	2.9 ± 0.66*	0.032	1.27	4.53
Silver-NPs	20 μg/mL	4.03 ± 0.29*	0.001	3.32	4.75
	40 μg/mL	4.83 ± 0.25*	0.0001	4.21	5.46
MMC	0.1 μg/mL	7.67 ± 0.72*	0.0001		

The increase in MNF was not found to be dose-dependent at 40 μg/mL exposure. This may be due to the increases in cell death caused by the high concentration of toxic particles. These results suggested that silver-NPs may induce chromosome damage in primary SHE cells.

3.4. Cell Cycle and Apoptosis

Cell cycle analysis was performed after exposing the SHE cells to 20 μg/mL silver-NPs. The cell cycle and proliferation index (PI) were estimated from the ratio of the S phase, the $G2/M$ phase, and the whole cell cycle using the following formula: $PI = (S + G2/M)/(G0/G1 + S + G2/M)$ at a cell proliferation rate of $PI \times 100\%$ (Table II).

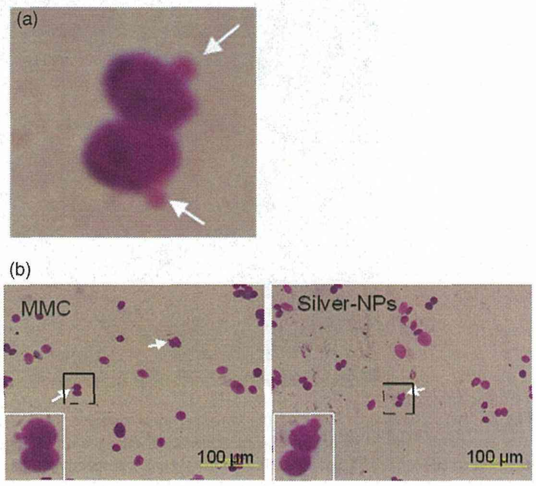

Fig. 3. Giemsa staining of SHE cells treated with MMC (positive control) and silver-NPs. Arrows indicate micronuclei in binucleated cells. (a) Typical micronucleus image in binucleated cell (MMC treatment culture). (b) Positive control (MMC) and silver-NP treatment. Images near the bottom of photo B are magnified micronuclei. Magnification: ×400.

Table II. Cell cycle and proliferation index (PI) of SHE cells exposed to silver-NPs at 20 μg/mL.

Groups	Time (h)	$G0/G1$ (%)	$G2/M$ (%)	S (%)	PI (%)*
Control	4	44.82	43.32	11.86	56.41
	8	47.42	43.05	9.53	53.68
	12	49.51	43.36	7.14	51.51
	24	50.11	39.66	10.24	50.89
	48	68.02	27.90	4.08	32.44
Silver-NPs	4	46.33	41.39	12.28	54.83
	8	64.44	21.54	14.03	36.11
	12	56.03	38.84	5.14	44.76
	24	56.50	32.40	11.11	44.28
	48	76.25	18.82	4.94	24.07

Notes: *PI represents the ratio between the S phase, the $G2/M$phase, and the whole cell cycle. $PI = (S+G2/M)/(G0/G1+S+G2/M)$; cell proliferation rate = $PI \times 100\%$.

The $G0/G1$ phase was found to be dominant after 8 h exposure, and the S phase was found to be significantly shorter than in untreated control cells, indicating that silver-NPs can arrest the cell cycle during the $G0/G1$ phase in primary SHE cells, and inhibit DNA replication and cell proliferation. The number of cells in the $G2/M$ phase was not found to be significantly different in cells exposed to silver-NPs and in control cells (Fig. 4).

The rate of late-stage apoptosis was lightly increased in the experimental groups than that in the control groups after 12 h exposure, and both early- and late-stage apoptosis were obviously increased after 72 h exposure (Fig. 5(A)–(B2)). These results suggested that apoptosis may play a role in cytotoxicity and genotoxicty of silver-NPs in primary SHE cells.

4. DISCUSSION

One previous study showed that silver-NP treatment can arrest the cell cycle in the $G(2)/M$ phase in U251 cells. This may be due to repair of damaged DNA.[21] In the present study, silver-NP exposure induced cell cycle arrest in the $G0/G1$ phase and significantly shortened the S phase after 8 h of exposure in primary SHE cells, indicating that DNA synthesis, not DNA repair, had been inhibited, and that this was what had inhibited cell proliferation. This cell cycle arrest resolved after 12 h exposure, and the cell cycle arrested in the $G0/G1$ phase was found again at 24 h and 48 h of exposure. This may indicate some cellular response to silver-NP exposure. It is also possible is that the cells had reached full confluence (data not shown) at 24 h or 48 h culture, and this may have caused the cells to cease proliferation. This conclusion is supported by the proliferation index (PI) which was very low in cells exposed to silver-NP exposure, as well as that in the control cells at 24 h and 48 h (Table II).

In this study, the rate of early-stage and late-stage apoptosis of SHE cells exposed to 20 μg/mL of silver-NPs were 6.64% and 8.21%, respectively, which obviously higher than the 3.97% and 4.93% observed in controls. Many studies have suggested that silver-NPs first affect the mitochondria and then basic cellular metabolism. Silver-NPs generate reactive oxygen species upon entering the cells, causing oxidative stress and mitochondrial toxicity.[32] In this study, MTT results, which indicate mitochondrial toxicity, show that the apoptosis induced by silver-NPs in SHE cells was mitochondrially mediated. The cytotoxicity of the silver-NPs, and their ability to induce apoptosis, is affected by particle size, morphology, surface modifications, charge, dispersion, agglomeration, and the type of cell exposed.[32–34] Some investigations have suggested that certain cancer cell lines might be more sensitive to silver-NP toxicity than normal cells and non-cancerous cell lines.[21,32] Mukherjee et al. found HeLa cells to be more sensitive than the HaCaT cells in *in vitro* assays.[32] HeLa cells are a cervical epithelial adenocarcinoma cell line, and HaCaT cells are an immortal non-cancerous human keratinocyte cell line. Mukherjee et al. believed that the

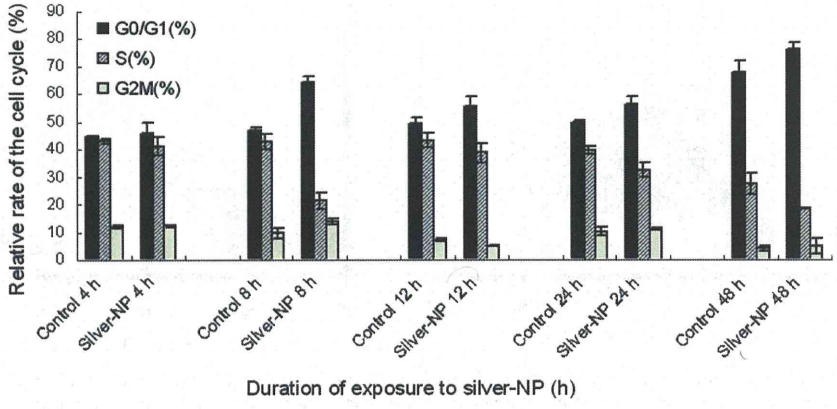

Fig. 4. Cell cycle analysis of SHE cells exposed to silver-NPs for different lengths of time. Data shown are the mean ± SD of three separate experiments. The counted cells containing the complete cell cycle ($GO/G1$, S, and $G2/M$) were taken to represent 100%.

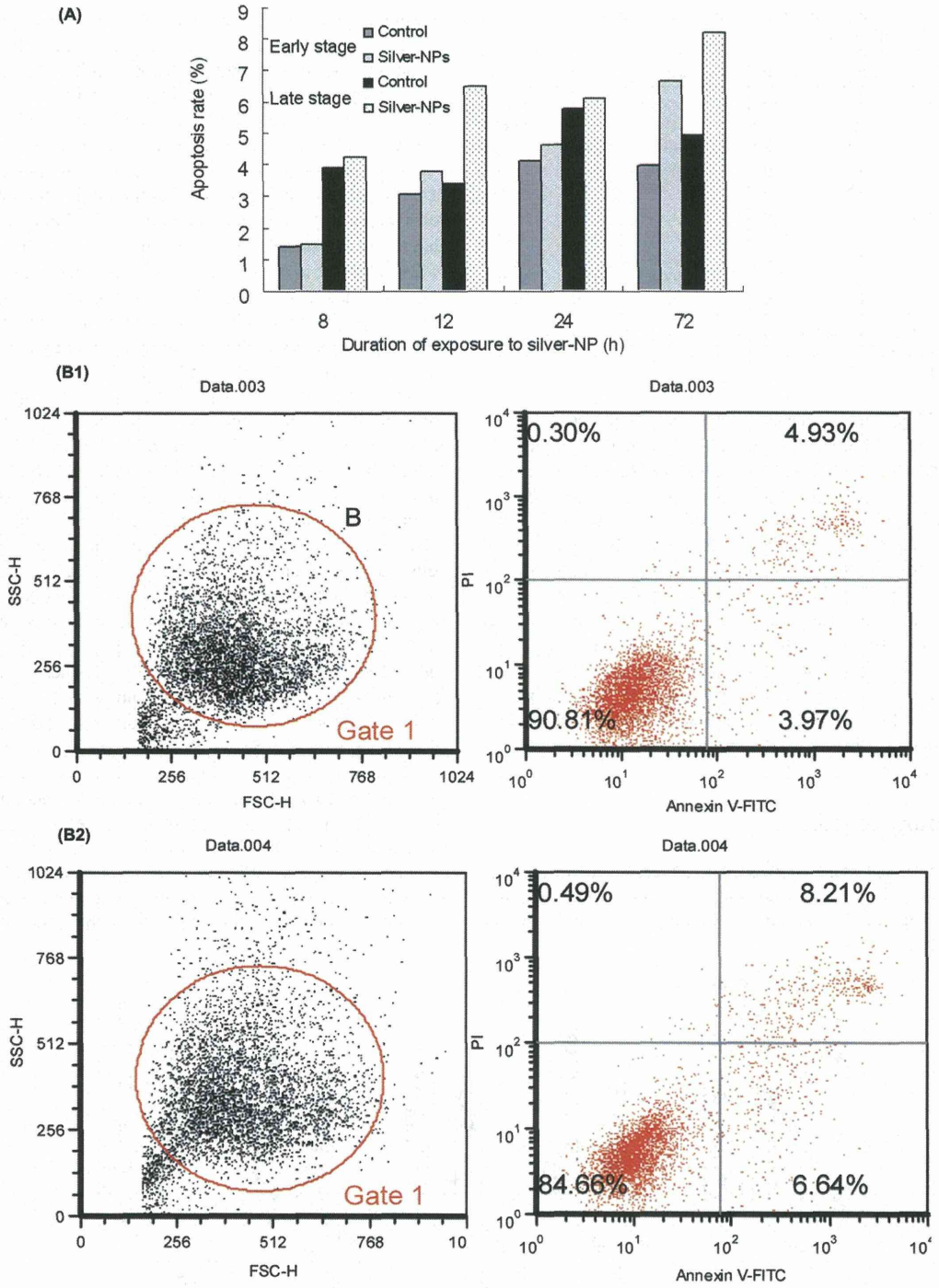

Fig. 5. (A) Rate of late- and early-stage apoptosis (%) among SHE cells in the control group and silver-NP groups (20 μg/mL). Data indicate the relative number of cells the in the gate. The total number of countable was taken as 100% level. Each silver-NP treatment group was compared to a control group that had been exposed to control substances for the same amount of time. The plots obtained using flow cytometric analysis indicated (B1) apoptosis in control cells and (B2) in cells exposed to silver-NP for 72 hours.

difference in the sensitivity of HaCaT and HeLa cells can be understood in terms of the difference in their natural antioxidant levels. In the present study, analysis of apoptosis did not involve comparisons to cancerous cells, but we believe that the normal cells are more suitable to assess toxicity, and more indicative of human cells *in vivo*.

CBMN assays are based on the blocking of cytokinesis by cytochalasin B (Cyt-B). In this way, chromosome damage events are detected only in dividing cells, which, unlike non-dividing cells, are can express the micronuclei produced in response to chromosome breakage or damage to the mitotic apparatus damage.[29–31] Cyt-B eliminates the confounding effect of altered cell division kinetics on micronuclear expression.[30] CBMN assays have been successfully applied to normal human lymphocytes, mouse spleen lymphocytes, mouse fibroblasts, and Chinese hamster lung fibroblasts.[30] In one previous study, a CBMN assay was successfully used on a human B lymphoblastoid cell line, and a significant increase in the frequency of micronucleated binucleation cells was observed when the cells were exposed to hydrogen peroxide or hypoxanthine (HX)/xanthine oxidase (XO), which generates superoxides.[31] In this way, CBMN assays are very sensitive to ROS-mediated DNA damage, making it very suitable for assessment of the nanomaterial-induced genotoxicity. In this study, a CBMN assay showed that silver-NPs at concentrations of 10, 20, and 40 μg/mL of silver-NPs (50.1% < 100 nm in size; 40.9% 100–200 nm; and 9% 818.4–1009.0 nm, as determined by DLS) induced significant increases in MNF in primary SHE cells ($P < 0.05$). Control cells showed a low MNF (1.6%). AshaRani and Hande et al. reported that exposure to 25 μg/ml silver-NPs (6–20 nm in size) induced chromosomal aberrations in 10% of normal IMR-90 cells (and in 0% of control cells) and in 20% of U251 cancer cells (and in 16% of control cells).[21] Kawata et al. showed that exposure to 1.0 μg/ml silver-NPs (7–10 nm in size) induced micronucleus formation in up to 47.9% of exposed HepG2 cells.[19] Hackenberg et al. reported that both a comet assay and chromosomal aberration test indicated DNA damage after 1, 3, and 24 h of exposure to 0.1 μg/mL silver nanoparticles in human mesenchymal stem cells.[35] These findings suggest that sensitivity to silver-NPs differs among cell types. It is likely that cancer cell lines may be more sensitive to genotoxicity than non-cancer cells and may have higher transformation backgrounds. Normal cells may more accurately reflect the exact genotoxicity of the test articles, as indicated in the present study, in which the transformation background of untreated SHE cells was very low (1.6%), as in IMR-90 cells (0%).[22]

To determine the genotoxic and carcinogenic risk of silver-NP in human cells, *in vivo* genotoxicity and carcinogenicity assessment is necessary. In one of our recent studies, vaginal exposure to silver-NP/Gel induced the formation of micronuclei, nuclear disruption, chromatin concentration, and apoptosis in rabbit reproductive organ tissues.[36] In the current study, the potential genotoxic and carcinogenic risk of nanomaterials was assessed on a case-by-case basis. Several studies have provided evidence of nano-specific genotoxicity and tumorigenicity, but other studies have not. This may be due to insufficient characterization of the test material, differences in experimental design, the use of different animal models and species, or differences in dosimetry and target organs.[3] As shown in Japan, it has taken about 10 years until finding that exposure to asbestos nanofibers can have serious carcinogenic effects.[37] Considering the rapid increase in the production and use of silver nanoparticles, it is imperative to gain a thorough understanding of their genotoxicity and carcinogenicity to prevent the human health catastrophe that resulted from widespread use of asbestos fibers.[37]

Acknowledgments: This study was financially supported by the Beijing Natural Science Foundation of China (No. 3112024); the Open Research Fund of State Key Laboratory of Bioelectronics, Southeast University, China (E04); National Key Technology Research and Development Program of the Ministry of Science and Technology of China (2012BAK26B00).

References and Notes

1. J. Zhao and V. J. Castranova, *Toxicol. Environ. Health Part B* 14, 593 (**2011**).
2. M. Ahamed, M. S. AlSalhi, and M. K. J. Siddiqui, *Clin. Chim. Acta* 411, 1841 (**2010**).
3. H. Becker, F. Herzberg, A. Schulte, and M. Kolossa-Gehring, *Int. J. Hyg. Environ. Health* 214, 231 (**2011**).
4. H. Tsuda, J. Xu, Y. Sakai, M. Futakuchi, and K. Fukamachi, *Asian Pac. J. Cancer Prev.* 10, 975 (**2009**).
5. T. M. Tolaymat, A. M. El Badawy, A. Genaidy, K. G. Scheckel, T. P. Luxton, and M. Suidan, *Sci. Total Environ.* 408, 999 (**2010**).
6. L. V. Stebounova, A. Adamcakova-Dodd, J. S. Kim, H. Park, P. T. O'Shaughnessy, V. Grassian and P. S. Thorne, *Part Fibre Toxicol.* 8, 5 (**2011**).
7. M. J. Piao, K. A. Kang, I. Lee, H. S. Kim, S. Kim, J. Y. Choi, J. Choi, and J. W. Hyun, *Toxicol. Lett.* 201, 92 (**2011**).
8. X. Chen and H. J. Schluesener, *Toxicol Lett.* 176, 1 (**2008**).
9. H. H. Lara, E. N. Garza-Treviño, L. Ixtepan-Turrent, and D. K. Singh, *J. Nanobiotechnology* 9, 30 (**2011**).
10. W. J. Yang, C. C. Shen, Q. H. An, J. J. Wang, Q. D. Liu, and Z. Z. Zhang, *Nanotechnology* 20, 085102 (**2009**).
11. G. A. Sotiriou and S. E. Pratsinis, *Environ. Sci. Technol.* 44, 5649 (**2010**).
12. K. Chaloupka, Y. Malam, and A. M. Seifalian, *Trends Biotechnol.* 28, 580 (**2010**).
13. L. Xu, T. Takemura, M. Xu, and N. Hanagata, *Materials Express* 1, 74 (**2011**).
14. L. Xu, X. Li, T. Takemura, N. Hanagata, G. Wu, and L. L. Chou, *J. Nanobiotechnology* 10, 16 (**2012**).
15. Y. S. Kim, M. Y. Song, J. D. Park, K. S. Song, H. R. Ryu, Y. H. Chung, H. K. Chang, J. H. Lee, K. H. Oh, B. J. Kelman, I. K. Hwang, and I. J. Yu, *Part. Fibre. Toxicol.* 7, 20 (**2010**).
16. J. Tang, L. Xiong, G. Zhou, S. Wang, J. Wang, L. Liu, J. Li, F. Yuan, and T. Xi, *J. Nanosci. Nanotechnol.* 9, 4924 (**2009**).

RESEARCH ARTICLE

17. J. Tang, L. Xiong, G. Zhou, S. Wang, J. Wang, L. Liu, J. Li, F. Yuan, S. Lu, Z. Wan, L. Chou, and T. Xi, *J. Nanosci. Nanotechnol.* 10, 6313 (**2010**).
18. J. S. Kim, J. H. Sung, J. H. Ji, K. S. Song, J. H. Lee, C. S. Kang, and I. J. Yu, *Saf. Health Work* 2, 34 (**2011**).
19. K. Kawata, M. Osawa, and S. Okabe, *Environ. Sci. Technol.* 43, 6046 (**2009**).
20. N. A. Flower, B. Brabu, M. Revathy, C. Gopalakrishnan, S. V. Raja, S. S. Murugan, and T. S. Kumaravel, *Mutat. Res.* 742, 61 (**2012**).
21. P. V. AshaRani, M. P. Hande, and S. Valiyaveettil, *BMC Cell Biology* 10, 65 (**2009**).
22. P. V. AshaRani, M. Low Kah Mun, M. P. Hande, and S. Valiyaveettil, *ACS Nano.* 3, 279 (**2009**).
23. J. H. Sung, J. H. Ji, K. S. Song, J. H. Lee, K. H. Choi, S. H. Lee, and I. J. YU, *Toxicol. Ind. Health* 27, 149 (**2011**).
24. R. Foldbjerg, D. A. Dang, and H. Autrup, *Arch. Toxicol.* 85, 743 (**2011**).
25. C. Carlson, S. M. Hussain, A. M. Schrand, L. K. Braydich-Stolle, K. L. Hess, R. L. Jones, and J. J. Schlager, *J. Phys. Chem.* 112, 13608 (**2008**).
26. Y. H. Hsin, C. F. Chen, S. Huang, T. S. Shih, P. S. Lai, and P. J. Chueh, *Toxicol. Lett.* 197, 130 (**2008**).
27. M. Valko, C. J. Rhodes, J. Moncol, M. Izakovic, and M. Mazur, *Chem. Biol. Interact.* 160, 1 (**2006**).
28. M. F. Rahman, J. Wang, T. A. Patterson, U. T. Saini, B. L. Robinson, G. D. Newport, R. C. Murdock, J. J. Schlager, S. M. Hussain, and S. F. Ali, *Toxicol. Lett.* 187, 15 (**2009**).
29. M. Fenech, *Environ. Health Perspect.* 101, 101 (**1993**).
30. M. Fenech, *Mutat. Res.* 392, 11 (**1997**).
31. M. Fenech, *Mutat. Res.* 455, 81 (**2000**).
32. S. G. Mukherjee, N. O'Claonadh, A. Casey, and G. Chambers. *Toxicology In Vitro* 26, 238 (**2012**).
33. A. M. El Badawy, R. G. Silva, B. Morris, K. G. Scheckel, M. T. Suidan, and T. M. Tolaymat. *Environ. Sci. Technol.* 45, 283 (**2011**).
34. P. W. Li, T. H. Kuo, J. H. Chang, J. M. Yeh, and W. H. Chan. *Toxicol. Lett.* 197, 8 (**2010**).
35. S. Hackenberg, A. Scherzed, M. Kessler, S. Hummel, A. Technau, K. Froelich, C. Ginzkey, C. Koehler, R. Hagen, and N. Kleinsasser, *Toxicol. Lett.* 201, 27 (**2011**).
36. L. Xu, L. Chen, Z, Dong, J. Wang, Z. Wang, and A. Shao, *Chi. J. Pharm. Anal.* 2, 33 (**2012**).
37. V. C. Sanchez, J. R. Pietruska, N. R. Miselis, R. H. Hurt, and A. B. Kane, *Wiley Interdiscip. Rev. Nanomed. Nanobiotechnol.* 1, 511 (**2009**).

Received: 6 February 2012. Accepted: 7 November 2012.

RESEARCH ARTICLE

Nanoscale

RSC Publishing

PAPER

Challenge to assess the toxic contribution of metal cation released from nanomaterials for nanotoxicology – the case of ZnO nanoparticles†

Cite this: *Nanoscale*, 2013, **5**, 4763

Mingsheng Xu,*[a] Jie Li,[b] Nobutaka Hanagata,[b] Huanxing Su,[c] Hongzheng Chen[a] and Daisuke Fujita[d]

The identification of physicochemical factors that govern toxic effects of nanomaterials (NMs) is important for the safe design and synthesis of NMs. The release of metal cations from NMs in cell culture medium and the role of the metal cations in cytotoxicity are still under dispute. Here, we report that removal of NMs such as ZnO nanoparticles (NPs) by centrifugation, the procedure commonly used for the estimation of released ion concentration in nanotoxicology, was incomplete even at a relative centrifugal force of 150 000 × *g*. In this sense, the Zn concentration in supernatant measured by inductively coupled plasma-mass spectrometry cannot be regarded as the concentration of free Zn^{2+} ions which were released from ZnO NPs in cell culture medium. This suggests the urgent need to develop relevant analytical techniques for nanotoxicology. The toxic contribution of released Zn^{2+} ions to the A549 cell lines was estimated to be only about 10%. We conclude that the cytotoxicity associated with ZnO NPs is not a function of the Zn concentration, suggesting that other factors play an important role in the toxic effect of ZnO NPs.

Received 23rd December 2012
Accepted 17th March 2013

DOI: 10.1039/c3nr34251d

www.rsc.org/nanoscale

1 Introduction

Novel nanomaterials (NMs) are playing key roles in nanotechnology innovations. However, the increasing use of NMs in industrial and consumer products has aroused global concern regarding their potential impact on the environment, human health, and society (NanoEHS). A number of studies on the effects of NMs in *in vitro* and *in vivo* systems have been published,[1,2] and showed that NMs including carbon nanotubes, fullerenes, quantum dots[3] such as CdS, oxide nanoparticles (NPs) such as ZnO, CuO and TiO_2, exhibited various toxic effects on biological systems. Despite the rapid growth of publications associated with NanoEHS recently, there are still many challenges and issues,[4,5] in particular on identifying toxic origins. The identification of physicochemical factors that govern the toxic effects of NMs is important for the safe design and synthesis of NMs and their applications. NMs do not behave in solution as inert objects or soluble small molecules. They often undergo aggregation or agglomeration,[6,7] dissolution processes,[8] and/or adsorption of proteins[9] or ions[10] from biological environments, leading to the formation of new entities.[10]

Many studies had attributed the toxic effects of metal-based NPs (NPs) primarily to released metal cations.[11] For example, Zn^{2+} ions were assumed to be released from ZnO particles as they were dispersed into cell culture medium or outside cells.[8,12–14] It was reported that the dissolution of ZnO NPs could occur in culture medium and reach >80% of the maximum total concentration of dissolved Zn^{2+} ions within 3 h; cell cultures were thus exposed mainly to aqueous Zn^{2+} ions when less than maximum concentrations of ZnO NPs were used.[8] Consequently, the toxic effect of ZnO NPs was mainly attributed to the dissolved Zn^{2+} ions in the cell culture medium.[8,11] By contrast, it was demonstrated that ZnO nanowires were comparatively stable in extracellular medium (pH = 7.4) and dissolution was low.[15] It was also confirmed by Gilbert *et al.*[16] that the majority of ZnO NPs did not dissolve in bronchial epithelial growth medium (BEGM). Furthermore, it was clearly shown that the toxicity of ZnO NPs to human colon-derived RKO cells was independent of the amount of soluble Zn^{2+} ions in the cell culture medium.[17] In the case of CuO NPs, there are also contradicting reports of the contribution of released Cu^{2+} to the observed toxicity.[18,19] The adverse biological effects of CuO NMs were explained by their solubility[20] based on the data obtained by the measurement using inductively coupled plasma-mass

[a]*State Key Laboratory of Silicon Materials, MOE Key Laboratory of Macromolecular Synthesis and Functionalization, Department of Polymer Science and Engineering, Zhejiang University, Hangzhou 310027, P. R. China. E-mail: msxu@zju.edu.cn*

[b]*Interdisciplinary Laboratory for Nanoscale Science and Technology, National Institute for Materials Science, 1-2-1 Sengen, Tsukuba, Ibaraki 305-0047, Japan*

[c]*State Key Laboratory of Quality Research in Chinese Medicine, Institute of Chinese Medical Sciences, University of Macau, Macau SAR, China*

[d]*Advanced Key Technologies Research Division, Nano Characterization Unit, National Institute for Materials Science, 1-2-1 Sengen, Tsukuba, Ibaraki 305-0047, Japan*

† Electronic supplementary information (ESI) available: High-resolution TEM images of ZnO NPs observed in the collected supernatant, TEM image and EDS maps of DMEM with FBS, in which no ZnO NPs were dispersed, XRD pattern for ZnO NPs, hydrodynamic size of ZnO suspensions and supernatants collected from the suspensions. See DOI: 10.1039/c3nr34251d

spectrometry (ICP-MS) relevant techniques or by the simple comparable toxicity to Cu salts[19,21] such as $CuSO_4$. By contrast, it was reported that cytotoxic effects related to the released copper fraction were found to be significantly lower than the effects related to CuO particles.[22,23] Thus, the link of free metal cations liberated from NPs to the observed toxicity or the toxic origin of NPs remains unclear.[19] In all these investigations,[8,12–14,19,20,22–24] the "free ion concentration" was commonly determined by using ICP-MS relevant techniques[25,26] to measure the supernatant collected after the nanomaterial suspension was centrifuged (Fig. 1). However, no study had addressed an important question – can centrifugation completely remove non-dissolved NMs from the suspension? The absence of an analytical technique for measuring the released metallic ion concentration makes it challenging to address the toxic contribution of released metal cations from NMs.

Here, we investigate the effectiveness of centrifugation on the removal of NMs from cell culture medium and the resultant impact on both the estimation of metal cation concentration and its toxic contribution. Our results show that the centrifugation process was unable to completely remove NPs even at very harsh centrifugation conditions, and thus it is not suitable to assume the elemental concentration measured by ICP-MS relevant techniques as the free ions in the suspension of NPs. Our study shows that the cytotoxicity associated with ZnO NPs is not a function of the Zn concentration. The estimated toxic contribution of released Zn^{2+} ions to the A549 cell line is only about 10%. These results shed light on how to evaluate metal cations released from NPs in cell culture medium and its contribution to cytotoxicity.

2 Materials and methods

2.1 Nanoparticles

High-purity ZnO and Al-doped ZnO (elemental Al content of about 3.4%) NPs were obtained from Sigma-Aldrich (Sigma-Aldrich Co., Japan). The primary dimensions and sizes of the oxides were provided in the data sheet, as determined by X-ray diffraction (XRD) and Brunauer–Emmett–Teller (BET) analysis. The average primary sizes of the ZnO and Al-doped ZnO NPs were about 60 nm and 50 nm, respectively, but were not uniform, as previously observed by electron microscopy.[27] We characterized the primary size, shape, and composition of the NPs by scanning electron microscopy (SEM) equipped with energy dispersive spectroscopy (EDS) (JSM-7001F, JEOL Inc., Japan) and by X-ray photoelectron spectroscopy (XPS) (PHI Quantera SXM, ULVAC-PHI, Japan).[27] We also used ZnO NPs with average size of about 20 nm for a comparative study. If not specifically stated, the ZnO NPs in this article are the ZnO NPs with average size of about 60 nm.

2.2 Nanoparticle suspension preparation

The cell culture medium was high-glucose Dulbecco's modified Eagle's medium (DMEM) (pH = 7.4) (Invitrogen) supplemented with 100 units mL^{-1} penicillin and 100 μg mL^{-1} streptomycin, which is simply called as DMEM in the present work. ZnO and Al-doped ZnO NPs were dispersed in the DMEM with or without 10% (v/v) fetal bovine serum (FBS) (SAFC Bioscience Inc.). The concentration of the NP suspensions was 25 μg mL^{-1} or 50 μg mL^{-1}.

2.3 Centrifugation process

The centrifugation of NP suspensions was carried out at 20 000 × *g* or 150 000 × *g* for different periods of time using the Optima LE-80 K Ultracentrifuge (Beckman Coulter, Brea, CA, USA). After centrifugation, the supernatant was collected carefully for use.

2.4 Transmission electron microscopy

The dark-field TEM images, high-resolution TEM (HRTEM) images, elemental mapping, and EDS spectra were analyzed using a JEM-2100F high-resolution transmission electron microscope (JEOL Inc., Japan) with an acceleration voltage of 200 kV.[10] The samples for TEM observation were prepared by

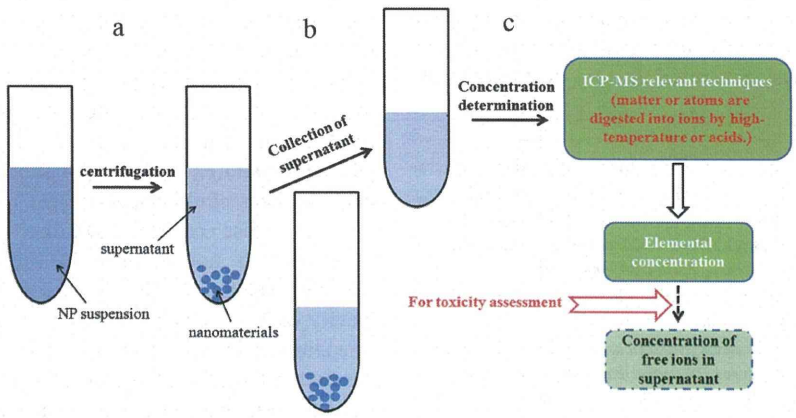

Fig. 1 Schematic diagram showing procedures to measure elemental concentration for toxicity evaluation of the contribution of free metal ions. (a) Centrifugation of nanomaterial suspension. (b) Collection of supernatant for ICP-MS measurement. (c) Measurement of elemental concentration by ICP-MS, and assuming the elemental concentration as the concentration of free ions in the supernatant.

immersing a TEM mesh into the supernatant collected after centrifugation of the suspension of ZnO NPs (25 μg mL^{-1}) for 24 h at 37 °C in the dark with 5% CO_2, that is, the same environment as for cell culture. After being dried in air, the TEM mesh was observed. We also carried out control experiments where TEM mesh was immersed into medium with FBS but without ZnO NPs (see ESI, Fig. S1 and S2†).

2.5 Hydrodynamic size distribution

The dynamic size of the ZnO (25 μg mL^{-1}) in DMEM with or without FBS and the collected supernatants was measured using a dynamic light scattering spectrophotometer (DLS-6000 AL; Otsuka Electronics, Japan). The DLS data indicate whether or not the suspensions or supernatants contain NPs. For a comparison, no particle was detected in the control sample of the medium with FBS, which suggests that the proteins in the solution did not form sediments under the experimental conditions. All the samples were measured at room temperature and were not incubated at 37 °C in the dark with 5% CO_2 prior to the characterization. This is different from the preparation of samples for TEM characterization because we found that the incubation of cell culture media with FBS in the culture environment leads to formation of particle-shaped matter[10] and in turn influences the DLS analysis. We had no intention to measure the accurate size distribution of the ZnO in these solutions by the DLS technique.

2.6 Elemental Zn concentration

The concentration of elemental Zn in the collected supernatants, ZnO suspensions, and Al-doped ZnO suspensions was measured by using inductively coupled plasma-optical emission spectrometry (SPS1700HVR, Seiko Instruments Inc., Japan). Before the measurements, 10% solutions of the samples were prepared with de-ionized water. The wavelengths used for Zn and Al analysis were 213.9 nm and 396.3 nm, respectively. The provided data were averaged from 3 measurements.

2.7 Viability of the A549 cell line

A549 cell lines were cultured in DMEM with or without FBS and grown in the dark at 37 °C in a 5% CO_2 humidified environment. Cells were seeded into a 3.9 cm^2 dish with a density of about 11 000 cells per cm^2. The cells were allowed to adhere for 24 h, followed by dilution of freshly dispersed nano-oxide suspensions (in sterilized, de-ionized water) into DMEM with or without FBS. After centrifugation of the ZnO suspension at 20 000 × *g* for 20 min, the supernatants were collected and immediately applied to the cells by replacing the old medium after dispersing for approximately 1 min using an Ecan Tube-Mixer (TM-2000, Asahi Techno Glass, Chiba, Japan). In the absence of ZnO NPs, control cells were cultured in the same volume of medium with or without FBS. The concentration dependence of ZnO NP suspensions on A549 cell viability was also investigated.

A calcein-AM staining kit (Dojindo Molecular Technologies Inc., Japan) was used to stain viable cells to assess A549 viability[27] after 24 h exposure to ZnO suspensions and supernatants. Before staining, the cells were washed twice with PBS. After staining, the cells were placed in an incubator for 10 min. Fluorescence images were then acquired using an inverted fluorescence microscope (DM2500 Fluo/PH, Leica Microsystems, Germany). We analyzed at least eight fields of cells in each dish, and used the averages of the data. Each experiment was carried out independently in triplicate. For statistical analysis, a two-tailed Student's *t*-test was performed. The result of this test was expressed as relative cell viability, which was calculated by [test]/[control], and the mean ± SEM (standard error of the mean) of three independent experiments. Results were considered statistically significant at $p < 0.05$.

3 Results and discussion

3.1 Supernatant containing ZnO NPs

Previously, we had characterized the NPs dispersed in different solvents in details;[27] and we found that the NPs can selectively adsorb various components from biological environments and in turn form bio-nanoparticle complexes.[10] Here, we use high-resolution TEM and ICP-OES to determine whether centrifugation can completely remove non-dissolved ZnO NPs from cell culture medium. Fig. 2 shows typical TEM images of the supernatant of ZnO NPs dispersed in DMEM with FBS collected after centrifugation at 20 000 × *g* for 20 min. We also carried out control experiments where a TEM mesh was immersed into DMEM with FBS but without ZnO NPs (see ESI, Fig. S1 and S2†).

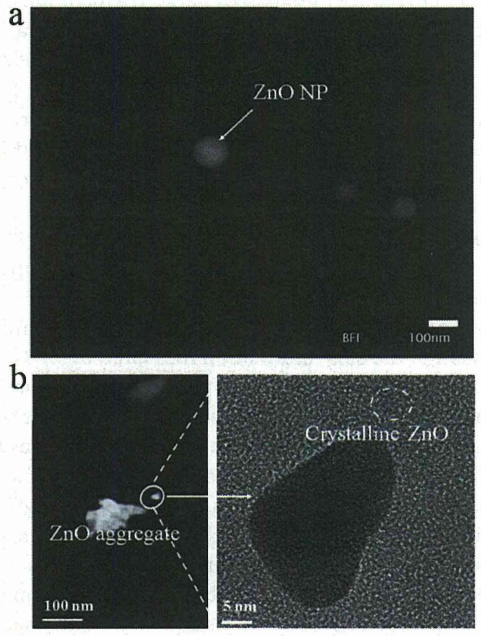

Fig. 2 ZnO NPs remained in the supernatant. (a) Dark-field TEM image. (b) Dark-field low magnification TEM image and high-resolution TEM images. The images were obtained from supernatant collected after centrifugation of the ZnO suspension in medium with fetal bovine serum, showing that crystalline ZnO is observed not only at the core region, but also in the shell region. The results suggest that centrifugation cannot completely remove the NPs from the suspensions.

We clearly observed highly ordered crystalline structures in the supernatant sample collected after centrifugation of the ZnO suspension (see ESI, Fig. S3†), but no crystalline structure was detected in the controls, in which the solution did not contain ZnO NPs. Together with X-ray diffraction (XRD) characteristics of the ZnO NPs (see ESI, Fig. S4†) and the EDS elemental mapping in ref. 10, these data indicate that the highly ordered structures are the ZnO NPs contained in the supernatant; individual ZnO NPs (Fig. 2b and ESI, Fig. S3†) are even embedded inside the clusters formed by ZnO NPs adsorbing various components from the biological environment.

In addition, we detected particles with different sizes in the supernatants collected after various centrifugation conditions, including the very harsh centrifugation conditions of 150 000 × *g* for 60 min (see ESI, Table S1†), by DLS measurement. For a control DLS measurement, we did not detect any particle in the solvents used for dispersing NPs at room temperature, suggesting that no protein sediment was formed under the experimental conditions (see ESI, Table S1†). Note that if the medium with FBS is incubated in a cell culture environment, particle-shaped matters can be formed (see ESI, Fig. S1†), and thus can influence the size distribution of NMs characterized by DLS. From the DLS results, clusters as large as 1.6 μm even existed in the supernatant generated at 20 000 × *g* for 20 min. It is well known that DLS measures the Brownian motion of NPs and relates this movement to an equivalent hydrodynamic diameter, with the motion of smaller particles not being easily detected or being overestimated. The measurement data are also influenced by time-dependent sedimentation and agglomeration/aggregation of NPs in order to reduce the surface energy in a medium. DLS is an indirect method for calculation of size by means of a physical model. This requires information on the refractive index of the dispersant in which the NMs are dispersed. Such a refractive index is now absent. All these factors suggest that the calculated equivalent hydrodynamic diameters are not compared with the particle sizes measured by TEM. Despite the problem of the DLS technique, our results suggest the presence of ZnO NPs in the supernatants. On the other hand, different from the DLS data, the maximum size of ZnO remaining in the supernatant observed by TEM is only around 100 nm, and only a few of such-sized clusters were found by searching the whole sample. The comparison of the size information measured by DLS and TEM suggests that the different size results can be obtained by different analytical techniques. Furthermore, the observation of remaining ZnO particles of size up to 100 nm indicates that the ZnO NPs in the supernatant may not be the portion of very small ZnO particles in the suspension. Despite the origin of the remaining ZnO clusters from either small particles or large clusters, their existence in the supernatant suggests that the ZnO NPs were not completely removed by the centrifugation process, which was at much harsher conditions than those used for the estimation of released metallic ions.[8]

3.2 Zn elemental concentration in supernatant

Zn concentrations of the supernatants produced by different centrifugation conditions were measured by using ICP-OES. As summarized in Table 1, the percentage of NPs removed from a suspension is dependent more on the relative centrifugal force than on centrifugation time. In the case of 60 nm sized ZnO NPs, at a relative centrifugal force of 20 000 × *g*, about 23.6% of the ZnO NPs were removed from a 25 μg mL^{-1} suspension, while 34.1% were removed at 150 000 × *g*. Extending the centrifugation time from 20 to 60 min at either 20 000 × *g* or 150 000 × *g* did not significantly change the percentage of ZnO NPs removed from the suspension. For instance, the Zn concentrations of the supernatants collected after centrifugation of the initial ZnO suspension for 20 min and 60 min at 20 000 × *g* were 16.8 and 16.9 ppm, respectively. However, the fraction removed at a fixed centrifugation time and fixed centrifugal force depended on the initial concentration of the nanoparticle suspension. About 50% of the ZnO NPs were removed from the 50 μg mL^{-1} suspension, which might be due to easy aggregation at a higher concentration to form larger aggregates. We obtained similar results to the 60 nm sized ZnO NPs when the 20 nm sized ZnO NPs were used for investigation. For both 60 nm and 20 nm sized ZnO NPs, we also studied the influence of FBS on the concentration of elemental Zn in the supernatant (Table 1), and found that the FBS with a volume ratio of 10% to the medium had no obvious effect on the removal of ZnO NPs.

In previous nanotoxicity studies that accounted for the metallic ion effect on cytotoxicity,[8,12–14,19,20,22–24] the elemental Zn concentration of supernatant obtained by ICP-MS relevant techniques was assumed to be the free Zn^{2+} ion concentration released in cell culture medium. However, it should be noted that the elemental concentration obtained by ICP-MS relevant techniques[25,26] can be affected by free ions and by the ions that result from decomposition of matter at the very high temperature and/or acid environments present for an ICP-MS measurement. That is, after the sample is injected for ICP-MS measurement, the plasma's extreme temperature or strong acid causes the sample to separate into individual atoms (atomization); and then these atoms are ionized ($M \rightarrow M^{+} + e^{-}$) so that they can be detected by the mass spectrometer. As a result, the digestion procedures involved in ICP-MS relevant techniques make it almost impossible to differentiate the ions formed as a result of nanomaterial dissolution from the NMs *per se*. Therefore, our TEM observation (Fig. 2) and DLS result (see ESI, Tables S1 and S2†) clearly suggest that the Zn concentration as measured by ICP-MS relevant techniques cannot be considered to be the actual concentration of free Zn^{2+} ions released in cell culture medium, as the centrifugation process does not completely remove ZnO NPs from the suspension. Our finding suggests the urgent need to establish relevant characterization method for accurate measurement of free ions in solution for toxicity study.

3.3 Toxic contribution of potentially released Zn^{2+}

To evaluate the toxicity of Zn^{2+} ions released into the cell culture medium, we investigated the viability of A549 cells after exposure to the supernatant collected after centrifugation of the ZnO suspension in medium containing FBS. We first investigated

